*Reprinted from*

JOURNAL OF THE PHYSICAL SOCIETY OF JAPAN

JOURNAL OF THE PHYSICAL SOCIETY OF JAPAN

http://jpsj.ipap.jp/

FULL PAPER

# Magnetic Excitations in Infinite-Layer Antiferromagnetic Insulator

Keisuke TOMIYASU, Hiroshi KAGEYAMA, Changhoon LEE, Mike H. WHANGBO, Yoshihiro TSUJIMOTO, Kazuyoshi YOSHIMURA, Jon W. TAYLOR, Anna LLOBET, Frans TROUW, Kazuhisa KAKURAI, and Kazuyoshi YAMADA

J. Phys. Soc. Jpn. **79** (2010) 034707

Journal of the Physical Society of Japan
Vol. 79, No. 3, March, 2010, 034707


# Magnetic Excitations in Infinite-Layer Antiferromagnetic Insulator

Keisuke TOMIYASU*, Hiroshi KAGEYAMA[1], Changhoon LEE[2], Mike H. WHANGBO[2], Yoshihiro TSUJIMOTO[1], Kazuyoshi YOSHIMURA[1], Jon W. TAYLOR[3], Anna LLOBET[4], Frans TROUW[4], Kazuhisa KAKURAI[5], and Kazuyoshi YAMADA[6]

*Department of Physics, Tohoku University, Sendai 980-8578, Japan*
[1]*Department of Chemistry, Graduate School of Science, Kyoto University, Kyoto 606-8502, Japan*
[2]*Department of Chemistry, North Carolina State University, Ralleigh, NC 27695-8204, U.S.A.*
[3]*ISIS Facility, Rutherford Appleton Laboratory, Chilton, Didcot, OX11 0QX, U.K.*
[4]*LANSCE, Los Alamos National Laboratory, Los Alamos, NM 87545, U.S.A.*
[5]*Quantum Beam Science Directorate, Japan Atomic Energy Agency, Tokai, Ibaraki 319-1195, Japan*
[6]*WPI Advanced Institute for Materials Research, Tohoku University, Sendai 980-8577, Japan*

(Received December 2, 2009; accepted January 7, 2010; published March 10, 2010)

The magnetic excitations of an infinite-layer antiferromagnetic insulator $SrFeO_2$ were examined by powder inelastic neutron scattering to find dispersive magnetic excitations from ~15 up to 63 meV. The scattering intensity distribution is well described by a spin wave model, confirming that the out-of-plane direct Fe···Fe exchange is comparable in strength to the in-plane Fe–O–Fe superexchange. $SrFeO_2$ shows an additional magnetic excitation mode around 30 meV, which is suggestive of an orbital magnon arising from small orbital moment on $Fe^{2+}$ brought about by spin–orbit coupling.

KEYWORDS: spin wave, orbital wave, orbital angular momentum, Mott insulator
DOI: 10.1143/JPSJ.79.034707

## 1. Introduction

Recently, a new iron-based antiferromagnetic insulator $SrFeO_2$ ($Fe^{2+}$: $d^6$, $S = 2$) constructed from square-planar $FeO_4$ units was obtained.[1)] This material has the crystal structure in which $FeO_2$ layers of corner-sharing $FeO_4$ square-planes alternate with layers of Sr as shown in Fig. 1(a), and is isostructural with the infinite layer compound $(Sr_{1-x}Ca_x)CuO_2$.[2,3)] $SrFeO_2$ exhibits several unexpected structural and physical properties. Its antiferromagnetic transition temperature $T_N \simeq 473$ K is unusually high despite its two-dimensional layered structure,[1)] and its infinite layer structure with P4/mmm space group is robust against cation substitution ($Sr^{2+}/Ca^{2+}$) as well as against temperature.[4)] Furthermore, it undergoes a pressure-induced spin transition into an intermediate spin state with $S = 1$, which is accompanied by insulator-to-metal and antiferromagnet-to-ferromagnet transitions.[5)] Density functional calculations for $SrFeO_2$[6,7)] showed that the down-spin of the high-spin $Fe^{2+}$ occupies the nondegenerate $d_{z^2}$, which shows $L = 0$ for the $Fe^{2+}$ ions and explains why Jahn–Teller instability is absent in $SrFeO_2$, and that the direct Fe···Fe spin exchange between adjacent $FeO_2$ layers is strong, hence accounting for the high $T_N$[1)] and the unprecedented spin transition for a square-planar coordinate system.[5,8)] However, there has been no experimental verification of the three-dimensional magnetic character on the basis of magnetic excitation energy measurements. The magnetic susceptibility of $SrFeO_2$ has not been reported because it is unstable at temperatures above ~450 K and because as-prepared samples possess ferromagnetic impurities difficult to remove.[1)] In this paper, we show on the basis of powder inelastic neutron scattering measurements that the out-of-plane direct Fe···Fe exchange is comparable in strength to the in-plane Fe–O–Fe superexchange, and $SrFeO_2$ exhibits an additional magnetic excitation mode similar in nature to an orbital magnon proposed for a Mott insulator with unquenched orbital angular momentum.[9)]

## 2. Experiments and Computational Details

Neutron scattering experiments were performed using direct geometry chopper spectrometers Mari at ISIS (UK) and Pharos at LANSCE (USA) installed at their respective spallation neutron sources. The incident energies ($E_i$) were fixed at 120 and 240 meV in the Mari and Pharos experiments, respectively. The data shown in the inset in Fig. 1(d) were obtained using Pharos, while all other data were obtained using Mari. The energy resolution at elastic condition was approximately 3% for $E_i$ in both experiments. Powder samples of $SrFeO_2$ were synthesized in the manner described in ref. 1. The 33 g and 36 g samples of $SrFeO_2$ were used for the Mari and Pharos experiments, respectively. Each sample was wrapped in a thin aluminum foil, which was then enclosed with $^4$He exchange gas in an aluminum container, and set under the cold head of a closed-cycle $^4$He refrigerator.

To determine the preferred spin orientation in the antiferromagnetic ground state of $SrFeO_2$, we carried out density-functional calculations for the crystal structure at 10 K[1)] using the full-potential linearized augmented plane wave method encoded in the WIEN2k program package[10)] with the generalized gradient approximation (GGA)[11)] for the exchange–correlation functional, the on-site repulsion $U$[12)] on Fe to describe the strong electron correlation associated with the Fe 3$d$ states, and the spin–orbit coupling (SOC) on the Fe atom. Further details of our GGA+U+SOC calculations (with several $U$ values between 0.0 and 4.6 eV) are summarized in ref. 13.

## 3. Results

Figure 1(b) shows neutron scattering intensity distribution in the $(Q, E)$ space, $S(Q, E)$, measured at $T = 5$ K, where $Q$ is the magnitude of momentum transfer and $E$ is the energy transfer. The magnetic excitations, whose intensity becomes

*E-mail: tomiyasu@m.tains.tohoku.ac.jp

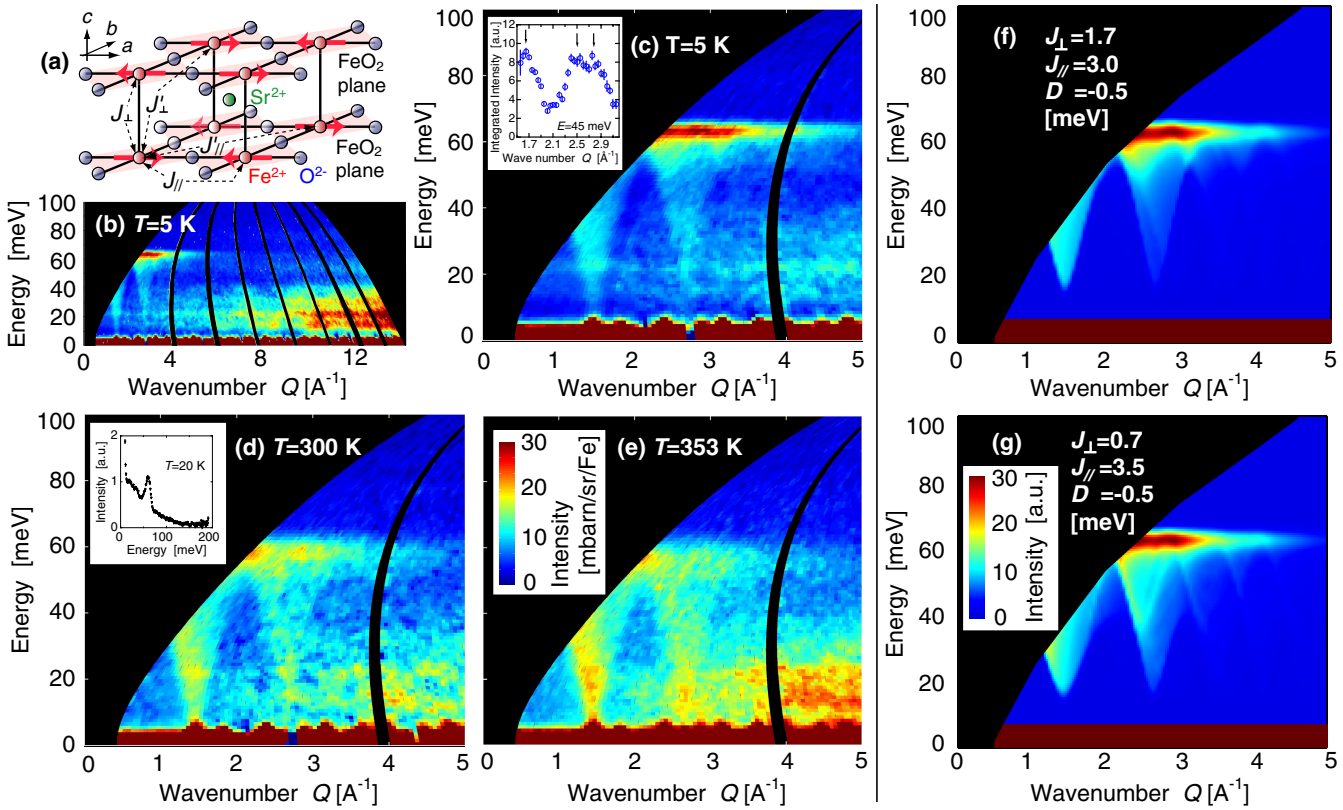


Fig. 1. (Color online) (a) Crystal and magnetic structures of $SrFeO_2$,[1)] where the solid arrows on the $Fe^{2+}$ ions indicate magnetic moments, which lie on the *ab* plane. The magnetic structure is represented by a propagation vector $(1/2, 1/2, 1/2)$. The dotted arrows define exchange interactions $J_\perp$, $J_\parallel$, $J'_\perp$, and $J'_\parallel$. (b–e) Experimental $S(Q,E)$ maps measured with $E_i = 120$ meV. The intensity tone is shown in the inset of (e). The inset of (c) shows the $Q$ dependence integrated from $E = 42$ to 48 meV, demonstrating the dispersion relation of the magnetic excitations. The inset of (d) shows the energy spectrum integrated from $Q = 0$ to 6 Å$^{-1}$ measured with $E_i = 240$ meV. (f,g) Calculated $S(Q,E)$ maps with $E_i = 120$ meV based on a spin wave model. (f) shows the best fit and (g) shows the map for a more two dimensional case ($E_\perp/E_\parallel = 0.1$). The intensity tone is shown in the inset of (g).

stronger in a lower $Q$ range, are observed, and the phonon density of states (nondispersive excitations), whose intensity becomes stronger in a higher $Q$ range, is distributed over the entire $Q$ region. Figure 1(c) magnifies the low $Q$ region in Fig. 1(b). Clear dispersive magnetic excitations are observed on the trail of the phonon density of states around 20 meV, which open up from energy minima located at $Q_c = 1.4$ and 2.7 Å$^{-1}$ to energy maximum ($E_t = 63$ meV) widely distributed in the $Q$ range. The positions of $Q_c$ correspond approximately to the magnetic Bragg points $(1/2, 1/2, 1/2)$ and $(3/2, 1/2, 1/2)$, consistent with the observed magnetic structure. In general, $S(Q,E)$ for a low-dimensional system is smeared along the $Q$ direction (e.g., see refs. 14 and 15). Thus the observed clear pattern qualitatively suggests a three-dimensional nature of the spin exchange interactions in $SrFeO_2$. The $Q$ dependence of the energy-integrated scattering intensity around $E_t$ [Fig. 2(a)] exhibits monotonic decrease up to ~5 Å$^{-1}$.

To estimate the energy minimum at $Q_c$, we roughly extracted the magnetic components:

$$S_{\mathrm{mag}}(E) = \int_{Q_c-0.4}^{Q_c+0.4} S(Q,E)\,\mathrm{d}Q - 2\left(\int_{Q_c-0.6}^{Q_c-0.4} S(Q,E)\,\mathrm{d}Q + \int_{Q_c+0.4}^{Q_c+0.6} S(Q,E)\,\mathrm{d}Q\right). \quad (1)$$

As seen in Fig. 1(b), the energy region below ~40 meV involves considerable phonon contributions. The $Q$ integrated range of the first term consists of both the magnetic excitations and phonons, while that of the second term can be regarded as the phonon background, as seen in Fig. 1(c). The first and second terms (S1 and S2) and their difference (S1 − S2) for $Q_c = 1.4$ Å$^{-1}$ are shown in Fig. 2(b). We confirmed that the $E$ dependence of S2 is almost the same as the phonon density of states obtained in the high $Q$ range in Fig. 1(b). In the S1 − S2, the peak structure of phonons disappears, indicating that no significant phonon contributions remain, and the energy minimum at $Q_c$ is estimated as $15 \pm 5$ meV, which corresponds to the gap energy ($E_g$).

Figures 1(d) and 1(e) show $S(Q,E)$ measured at $T = 300$ and 353 K, respectively. With increasing $T$, the intensity of the magnetic excitations in the energy range higher than $T$ (such as around $E_t$) decreases, while the opposite happens in the energy range lower than $T$ because of the Bose population factor.

## 4. Discussion

The magnetic excitation energies of $SrFeO_2$ can be described by the Heisenberg spin Hamiltonian,

$$H = \sum_{m,n} J_{mn} \boldsymbol{S}_m \cdot \boldsymbol{S}_n + D \sum_m (S_{mz})^2, \quad (2)$$

where $m$ and $n$ are $Fe^{2+}$ sites, the spin exchange parameters $J_{mn}$ are defined in Fig. 1(a), and $D$ is the spin anisotropy constant. The LDA (local density functional)+U calculations gave the estimates $(J_\perp, J_\parallel, J'_\perp, J'_\parallel) = (1.09, 3.52, -0.12,$

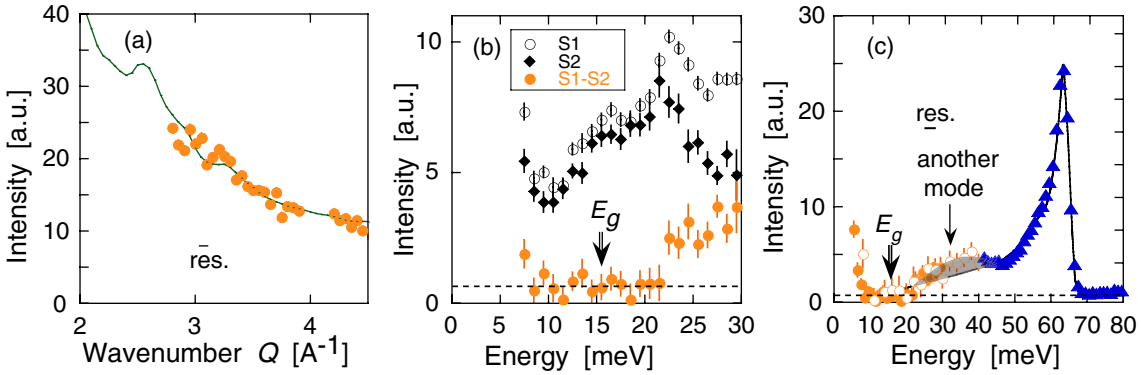


Fig. 2. (Color online) $Q$ dependence of the scattering intensity integrated from $E = 60$ to 66 meV (a), $Q$-integrated energy spectra around $Q_c = 1.4$ Å$^{-1}$ (b), and the comparison between with experimental magnetic energy spectrum and calculated spin-wave spectrum (c). The experimental (symbols) and calculated (solid lines) data are obtained from the data shown in Figs. 1(c) and 1(f), respectively. The dotted lines are guide for eyes. In (a), the experimental errors are smaller than the symbol sizes. In (b), S1 − S2 = $S_{mag}$, where S1 and S2 are the first and second terms in eq. (1), respectively. In (c), the solid and open circles correspond to S1 − S2 for $Q_c = 1.4$ and 2.7 Å$^{-1}$, respectively, and the solid triangles indicate the raw spectrum integrated from $Q = 0$ to 4 Å$^{-1}$ above $E \sim 40$ meV. The intensity scales of these three data sets, which are different because of a magnetic form factor, are adjusted to smoothly connect the data points. The gray shaded area suggests the existence of another magnetic mode.

0.22)[6] and $(J_\perp, J_\parallel, J'_\perp) = (0.88, 3.29, -0.13)$[7] in meV units. Xiang *et al.* found $D = -1.0$ meV from their LDA+U+SOC calculations for the ferromagnetic state of the optimized $SrFeO_2$ structure.[6] Our GGA+U+SOC calculations for the experimental $SrFeO_2$ structure show that $D = -0.45$ meV for the ferromagnetic state, and $D = -0.39$ meV for the antiferromagnetic state.

The ratio of the out-of-plane exchange to the in-plane energy, $E_\perp/E_\parallel \equiv \sum_{m,n_\perp}(J_{mn_\perp}S_{mz}S_{n_\perp z})/\sum_{m,n_\parallel}(J_{mn_\parallel}S_{mz}S_{n_\parallel z}) = (2J_\perp - 8J'_\perp)/(4J_\parallel - 4J'_\parallel)$, where $n_\perp$ and $n_\parallel$ mean the out-of-plane and in-plane $Fe^{2+}$ sites for a given $m$ site, respectively, is 0.23[6] and 0.21[7] for each set of the theoretical $J$ values. $E_\perp/E_\parallel$ is 0 for a completely two-dimensional system, and 0.5 for an isotropically three-dimensional system.

We analyze the $S(Q,E)$ data at $T = 5$ K [Fig. 1(c)] in terms of a spin wave model by using only $J_\perp$, $J_\parallel$, and $D$ in eq. (2). Then, the spin wave dispersion $\hbar\omega(\boldsymbol{q})$ for the propagation vector $\boldsymbol{q} = (q_a, q_b, q_c)$ can be described by the Holstein–Primakoff formalism

$$\hbar\omega(\boldsymbol{q}) = 2S\sqrt{[J_\perp(\boldsymbol{0}) + J_\parallel(\boldsymbol{0}) - D]^2 - [J_\perp(\boldsymbol{q}) + J_\parallel(\boldsymbol{q})]^2}, \quad (3)$$

where $S = 2$, $J_\perp(\boldsymbol{q}) = 2J_\perp \cos 2\pi q_c$, and $J_\parallel(\boldsymbol{q}) = 2J_\parallel(\cos 2\pi q_a + \cos 2\pi q_b)$. In terms of $\hbar\omega(\boldsymbol{q})$ the $S(Q,E)$ function can be written as

$$S(Q,E) = A\left\langle\sqrt{\frac{E_i - E}{E_i}}|F(\boldsymbol{Q})|^2(1+\cos^2\theta)|t(\boldsymbol{Q})|^2\delta[E - \hbar\omega(\boldsymbol{q})]\right\rangle, \quad (4)$$

where $A$ is a scale factor of the scattering intensity, $E_i = 120$ meV, $F(\boldsymbol{Q})$ is a magnetic form factor, $\boldsymbol{Q}$ is a scattering vector, $\theta$ is the angle between $\boldsymbol{Q}$ and $\boldsymbol{S}$ [the preferred spin orientation is parallel to the $a$ axis,[1,6] as shown in Fig. 1(a)], $t(\boldsymbol{Q})$ is a dynamic structure factor of the spin wave,[16] and $\langle\cdots\rangle$ represents powder orientational averaging. For the energy scale discussed in this study, the temperature factors are negligible at $T = 5$ K (∼0.4 meV).

Equation (3) shows that, if $D$ is nonzero, there exists an excitation energy gap $E_g$ given by $E_g = \hbar\omega(0)$. Using the experimentally obtained values $E_t = 63$ meV and $E_g = 15$ meV in eq. (3), $J_\perp = 7.65 - 2J_\parallel$ meV and $D = -0.5 \pm 0.3$ meV are obtained; this reduces the number of free parameters to only $J_\parallel$. For $F(\boldsymbol{Q})$, the Watson–Freeman form factor is used.[17] Then, by solving eq. (4), we obtain the best-fit shown in Fig. 1(f), which yields $(J_\perp, J_\parallel, D) = (3.0 \pm 0.2, 1.7 \mp 0.3, -0.5 \pm 0.3)$, in excellent agreement with the observed $S(Q,E)$ [Fig. 1(c)]. For a set of more two-dimensional parameters (i.e., with smaller $J_\perp/J_\parallel$ ratio), the pattern becomes smeared along the $Q$ direction as shown in Fig. 1(g). The $Q$ dependence around $E_t$ is also consistent with the experimental data [Fig. 2(a)]. Furthermore, the $E_t$ value decreases gradually by a few meV on going from Figs. 1(c) to 1(e). This decreasing is consistent with a spin wave, as found for MnO.[18,19]

The obtained ratio $J_\perp/J_\parallel = 0.57 \pm 0.14$ ($E_\perp/E_\parallel = 0.28 \pm 0.07$) demonstrates that the magnetism in $SrFeO_2$ is three dimensional. The theoretically obtained $J$ values[6,7] also exhibit the $S(Q,E)$ pattern similar to that shown in Fig. 1(f); the experimental $E_\perp/E_\parallel$ ratio agrees well with the theoretical one (0.23 and 0.21). The three dimensional magnetic character of $SrFeO_2$ reflects that the direct Fe···Fe exchange associated with the out-of-plane magnetic orbitals (i.e., the $d_{xz}$ and $d_{yz}$ orbitals) is substantial. In contrast, the isostructural compound $(Sr_{1-x}Ca_x)CuO_2$ ($Cu^{2+}$: $3d^9$, $S = 1/2$, $k_BT_N/E_\parallel \sim 0.1$)[20] has no three-dimensional character because its magnetic orbital Cu $3d_{x^2-y^2}$ possesses no out-of-plane character. The experimental value of $D$ (i.e., $-0.5 \pm 0.3$ meV) is in good agreement with the theoretical value estimated from the present GGA+U+SOC calculations for the antiferromagnetic state (i.e., −0.39 meV). The nonzero $D$ value arises from the SOC, which mixes the down-spin $d_{zx}$ and $d_{yz}$ orbital character into the down-spin $d_{z^2}$ orbital, hence leading to a small, nonzero orbital moment on $Fe^{2+}$ (of the order of 0.1 $\mu_B$ from the present GGA+U+SOC calculations).

Figure 2(c) shows the experimental energy spectrum of magnetic excitations (symbols) and the spin-wave density of states calculated by integrating the spin-wave scattering intensity over the whole Brillouin zone with resolution

correction (solid curve).[21] In this calculation, the scale factor was adjusted such that the intensity around $E_t$ coincides with the experimental data. As expected, the calculated spin-wave density of states is convex downward. However, the experimental data exhibits a broad convex-upward feature in the $E_{2nd} \sim 30$ meV region, which shows the presence of an additional magnetic excitation mode superposed on the spin wave in the $E_{2nd}$ region. This additional excitation mode cannot be related to the excitations between the crystal-field-split $d$-states, because the smallest excitation gap (from the down-spin $d_{z^2}$ to the down-spin $d_{xz}$ and $d_{yz}$ levels) is much greater than 0.1 eV from the density functional calculations.[6,7]

It is of interest to consider a probable cause for the additional magnetic excitation in the ~30 meV region. The single-crystal inelastic neutron scattering study[9] of the Mott-type antiferromagnetic insulator CoO with high-spin $Co^{2+}$ (effective $L = 1$, $S = 3/2$) ions showed that, in addition to the spin wave excitations with $E_g \sim 20$ meV and $E_t \sim 70$ meV, it exhibits excitations centered around $E_{2nd} \sim 40$ meV. The latter have been suggested to arise from an orbital magnon, i.e., a collective excitation in which the tilting of $\boldsymbol{L}$ is propagated like a spin wave.[9] The magnetic excitations of $SrFeO_2$ exhibit similar features. Namely, in addition to the spin wave excitations with $E_g \sim 15$ meV and $E_t \sim 63$ meV, it exhibits excitations centered around $E_{2nd} \sim 30$ meV. This similarity leads us to suggest that the additional excitations of $SrFeO_2$ centered around ~30 meV are due to an orbital magnon, although some phonon contributions to the ~30 meV excitations cannot be ruled out completely because unpolarized neutrons were used in our scattering experiments. Given that an orbital magnon mode can occur in $SrFeO_2$ with small orbital moment on $Fe^{2+}$ as well as in CoO with large unquenched orbital moment on $Co^{2+}$, it appears that orbital magnon is a universal phenomenon in magnetic insulators of 3$d$ magnetic ions with nonzero orbital moment.

## 5. Conclusions

In summary, our powder inelastic neutron scattering study confirms that $SrFeO_2$ has a three-dimensional magnetic character, and shows a magnetic excitation mode superposed on the spin wave in the ~30 meV region. The latter is suggestive of an orbital magnon, which arises from small orbital moment on $Fe^{2+}$ induced by SOC.

## Acknowledgment

This work was supported by Grants-in-Aid for Scientific Research on Priority Areas (19052004) and Scientific Research (B) and (S), Japan–UK Collaboration Program on Neutron Scattering, Quantum Beam Technology Program, World Premier International Research Center Initiative (WPI Initiative), the Ministry of Education, Culture, Sports, Science and Technology, Japan. This work has benefited from the use of Pharos at the Lujan Center at LANSCE, funded by DOE Office of Basic Energy Sciences. Los Alamos National Laboratory is operated by Los Alamos National Security LLC under DOE Contract DE-AC52-06NA25396. M.-H. W. thanks U.S. Department of Energy for the financial support (Grant No. DE-FG02-86ER45259). We thank Mr. Masaki Morita and Ms. Aya Sakaiguchi for assisting in the synthesis of samples.

1) Y. Tsujimoto, C. Tassel, N. Hayashi, T. Watanabe, H. Kageyama, K. Yoshimura, M. Takano, M. Ceretti, C. Ritter, and W. Paulus: Nature **450** (2007) 1062.
2) M. Takano, Y. Takeda, H. Okada, M. Miyamoto, and T. Kusaka: Physica C **159** (1989) 375.
3) M. Azuma, Z. Hiroi, M. Takano, Y. Bando, and Y. Takeda: Nature **356** (1992) 775.
4) C. Tassel, J. M. Pruneda, N. Hayashi, T. Watanabe, A. Kitada, Y. Tsujimoto, H. Kageyama, K. Yoshimura, M. Takano, M. Nishi, K. Ohoyama, M. Mizumaki, N. Kawamura, J. Iniguez, and E. Canadell: J. Am. Chem. Soc. **131** (2009) 221.
5) T. Kawakami, Y. Tsujimoto, H. Kageyama, X.-Q. Chen, C. L. Fu, C. Tassel, A. Kitada, S. Suto, K. Hirama, Y. Sekiya, Y. Makino, T. Okada, T. Yagi, N. Hayashi, K. Yoshimura, S. Nasu, R. Podloucky, and M. Takano: Nat. Chem. **1** (2009) 371.
6) H. J. Xiang, S.-H. Wei, and M.-H. Whangbo: Phys. Rev. Lett. **100** (2008) 167207.
7) J. M. Pruneda, J. Iniguez, E. Canadell, H. Kageyama, and M. Takano: Phys. Rev. B **78** (2008) 115101.
8) M.-H. Whangbo and J. Koehler: Nat. Chem. **1** (2009) 351.
9) K. Tomiyasu and S. Itoh: J. Phys. Soc. Jpn. **75** (2006) 084708.
10) P. Blaha, K. Schwarz, G. K. H. Masden, D. Kvasnicka, and J. Luitz: *Wien2k* (Vienna University of Technology, Vienna, 2001).
11) J. P. Perdew, K. Burke, and M. Ernzerhof: Phys. Rev. Lett. **77** (1996) 3865.
12) V. I. Anisimov, I. V. Solovyev, M. A. Korotin, M. T. Czyzyk, and G. A. Sawatzky: Phys. Rev. B **48** (1993) 16929.
13) Our GGA+U+SOC calculation employed the 64 $k$-points for the irreducible Brillouin zone, the threshold of $10^{-6}$ Ry for the energy convergence, $RK_{max} = 7.0$ and $G_{max} = 12$, and the energy threshold of $-6.0$ Ry for the separation of the core and valence states.
14) R. S. Eccleston, T. Barnes, J. Brody, and J. W. Johnson: Phys. Rev. Lett. **73** (1994) 2626.
15) S. J. Crowe, S. Majumdar, M. R. Lees, D. McK. Paul, R. I. Bewley, S. J. Levett, and C. Ritter: Phys. Rev. B **71** (2005) 224430.
16) G. Shirane, S. M. Shapiro, and J. M. Tranquada: *Neutron Scattering with a Triple-Axis Spectrometer: Basic Techniques* (Cambridge University Press, Cambridge, U.K., 2002), Chap. 5.
17) R. E. Watson and A. J. Freeman: Acta Crystallogr. **14** (1961) 27.
18) G. Pepy: J. Phys. Chem. Solids **35** (1974) 433.
19) M. Kohgi, Y. Ishikawa, I. Harada, and K. Motizuki: J. Phys. Soc. Jpn. **36** (1974) 112.
20) A. Keren, L. P. Le, G. M. Luke, B. J. Sternlieb, W. D. Wu, Y. J. Uemura, S. Tajima, and S. Uchida: Phys. Rev. B **48** (1993) 12926.
21) K. Tomiyasu and S. Itoh: Physica B **385** (2006) 1110.